Published in final edited form as:

Methods Cell Biol. 2013 ; 117: 359–371. doi:10.1016/B978-0-12-408143-7.00019-0.

Monitoring peripheral protein oligomerization on biological membranes

Robert V. Stahelin

Department of Biochemistry and Molecular Biology, Indiana University School of Medicine-South Bend, South Bend, IN 46617, USA and Department of Chemistry and Biochemistry, University of Notre Dame, Notre Dame, IN 46556, USA

Abstract

Peripheral proteins transiently interact with cellular membranes where they regulate important cellular events such as signal transduction. A number of peripheral proteins harbor lipid-binding modules that not only bind selectively with nanomolar affinity to biological membranes but also oligomerize on the membrane surface. In some cases specific lipid binding or specific lipid compositions can induce peripheral protein oligomerization on cellular membranes. These oligomers serve different roles in biological signaling such as regulating protein-protein interactions, induction of membrane bending, or facilitating membrane scission. A number of technologies have been employed to study protein oligomerization with fluctuation analysis of fluorescently labeled molecules recently developed for use with commercial laser scanning microscopes. In this chapter the approach of Raster Image Correlation Spectroscopy coupled with Number and Brightness (N&B) analysis to investigate protein oligomerization on cellular membranes in live cells is presented. Important considerations are discussed for designing experiments, collecting data, and performing analysis. N&B analysis provides a robust method for assessing membrane binding and assembly properties of peripheral proteins and lipid-binding modules.

Keywords

lipid binding; membrane binding; oligomerization; peripheral protein; protein assembly

I. Introduction

Fluctuation analysis has been used to monitor protein oligomerization (Barnwal *et al.*, 2011; Wang *et al.*, 2004) as it serves as the basis for dynamic light scattering and fluorescence correlation spectroscopy (FCS). While DLS requires many molecules to produce a signal, FCS can detect single molecules in complex mixtures such as live cells or solutions containing lipids and proteins. FCS was developed in the 1970s (Magde et al., 1972; 1974) and can detect fluctuation changes in fluorescence while characterizing molecular brightness of the particles. FCS has become more applicable to biologists and biochemists as its use was applied to live cell studies (Berland *et al.*, 1995; Schwille *et al.*, 1997; Schwille, 1999)

Address correspondence to: rstaheli@iupui.edu.

and more recently scanning confocal microscopes have been used (Digman *et al.* 2005a; 2005b). Fluorescence intensity fluctuations are often due to protein conformation changes, protein binding to immobile or less mobile fractions, or the entry and exit of molecules through the area being imaged. In FCS, a fixed observation volume is used to detect fluctuations in fluorescence intensity as single molecules pass through the detection area. However, FCS alone does not account for the location of fluorescent particles as a function of time so a spatial correlation approach can be used in order to associate changes in fluorescent amplitude at one spot with changes in nearby positions. A change in the correlation function of FCS can be performed with Raster image correlation spectroscopy (RICS) (Digman and Gratton, 2009; Digman *et al.*, 2013; Rossow *et al.*, 2010) where the position of the observation volume is changed with respect to time. This means that the correlation is dependent upon how fast the fluorescent molecules are moving as well as how fast the observation volume is changing in a time dependent manner.

RICS can be used to detect and measure fluorescent dynamics in complex environments such as the cellular cytoplasm and membrane organelles. While determination of protein oligomerization and protein complex stoichiometry is a challenging task in live cells, it is an important one as many biological processes often depend upon protein clustering (Choi *et al.*, 2011; Digman, *et al.*, 2008a; Digman *et al.*, 2009). Recently, determination of fluorescently labeled protein clustering has become much more robust with Number and Brightness (N&B) analysis (Digman et al., 2008). N&B analysis is based upon moment analysis and allows for measurement of the average number of molecules as well as brightness in each pixel of a fluorescent microscopy image (Digman *et al.*, 2008). N&B utilizes the first and second moment of amplitude fluctuations from the histogram of amplitude oscillations, which is originally derived from the photon counting histogram method (Chen *et al.*, 1999). The average brightness of a particle is determined from the ratio of variance to intensity at each pixel. Fluctuating particles can be determined by dividing the average intensity by the brightness at each pixel. For particles fluctuating in the focal volume, the variance is proportional to the square of the particle brightness; however, the variance of the immobile particles and detector noise is proportional to the intensity of these components. Thus, only fluorescent fluctuations that are dependent upon the mobile particles have a ratio of the variance to intensity > 1. Aggregation of mobile fluorescent particles can then be determined from a brightness map with pixel resolution.

For an electron multiplying CCD camera the following equations are used to compute the number and brightness.

$$N=(<I>-\text{offset})^2/(\sigma^2-{\sigma_0}^2) \quad (1)$$

$$B=(\sigma^2-{\sigma_0}^2)/(<I>-\text{offset}) \quad (2)$$

In these equations, N and B are the apparent number and the brightness of the molecule, $< I >$ is the average intensity of a pixel throughout a stack of frames (time average), σ^2 is the variance, while *offset* and ${\sigma_0}^2$ are properties that depend on the camera hardware. With these

parameters properly calibrated, the distribution of the brightness of each individual pixel in the image of a section of a cell can be investigated. This approach is therefore useful to study interactions of fluorescently labeled proteins that occur on cellular membranes.

Cellular membranes contain hundreds if not thousands of different lipids, which are highly dynamic. Specific lipids in the membrane bilayer (Lemmon, 2008; Stahelin, 2009) or lipid anionic charge (Yeung *et al.*, 2006) can regulate recruitment of peripheral proteins to the membrane interface. These signaling cues are vital to membrane trafficking and signal transduction as it is estimated that nearly half of all proteins in the human genome are localized in or on membranes. A large number of peripheral proteins are recruited to cellular membranes through modular lipid-binding domains that are often found in signal transduction and membrane trafficking proteins (Cho and Stahelin, 2005). These modular lipid-binding domains can bind, often with nanomolar affinity, to membranes containing a specific lipid ligand or recognize membrane physical properties such as charge or curvature (Lemmon, 2008). Binding to the membrane interface and restricting the protein to two dimensions reduces dimensionality and provides a platform for signal transduction to occur. In some cases peripheral proteins may interact or oligomerize on the membrane interface, an event that is important in biological processes such as generation of membrane curvature changes (Zimmerberg and Kozlov, 2006), membrane scission (Klein *et al.*, 1998; Ross *et al*., 2011), and assembly and egress of viral proteins from the host cell (Adu-Gyamfi *et al.*, 2012; Hoenen *et al.*, 2010; Murray *et al*., 2005). Because high affinity interactions between these peripheral proteins regulate lipid signaling and trafficking events from cellular membranes, accurately characterizing lipid specificity and membrane affinity can establish how the membrane-interface signals throughout the cell. Technologies aimed at measuring the assembly and stoichiometry of lipid-protein and protein-protein interactions on or near the membrane interface are important for revealing molecular details of the underlying cellular architecture.

The biophysical approaches discussed above have been applied to investigate the oligomerization state of the fission protein dynamin (Ross J.A. *et al.*, 2011) as well as oligomerization of the lipid binding ENTH (Yoon *et al*., 2010) and BAR (Yoon *et al*., 2012) domains involved in membrane curvature generation and sensing. Additionally, they have been useful in yielding mechanistic information of assembly and oligomerization of Annexin A4 (Crosby *et al.*, 2013), oligomerization of the voltage-dependent anion channel in response to phostphatidylglycerol binding (Betanelli *et al.*, 2012) as well as oligomerization, assembly, and egress of the Ebola virus matrix protein (Adu-Gyamfi *et al*., 2012, Adu-Gyamfi *et al.*, 2013, Soni *et al.*, 2013). In this chapter, I will describe how RICS and N&B can be used to study assembly of peripheral proteins on biological membranes.

II. Materials & Methods

A. Cell maintenance, Transfection, and Observation

Human Embryonic Kidney (HEK293) and Chinese Hamster Ovary-K1 (CHO-K1) cells were used to study the assembly and oligomerization of the Ebola virus matrix protein VP40 (Adu-Gyamfi *et al.*, 2012; Adu-Gyamfi *et al.*, 2013). HEK293 cells were cultured and maintained at 37°C in a 5% CO_2 humidified incubator supplemented with DMEM (low

glucose) containing 10% FBS and 1% Pen/Strep. After trypsinization, cells were transferred from a T-25 tissue culture flask to an 8-well plate used for imaging. Cells were then grown to 50–80% confluency and transfected with 1 μg DNA/dish using lipofectamine 2000 according to the manufacturer's protocol. Cells were imaged between 12 and 20 hours post transfection.

CHO-K1 cells were cultured and maintained at 37°C in a 5% CO_2 humidified incubator supplemented with DMEM/F12 (low glucose) containing 10% FBS and 1% Pen/Strep. After trypsinization, cells were transferred from a T-25 tissue culture flask to an 8-well plate used for imaging. Cells were then grown to 50–80% confluency and transfected with 1 μg DNA/dish using lipofectamine LTX according to the manufacturer's protocol. Both HEK293 and CHOK-1 cells were imaged using a Zeiss LSM 710 confocal microscope using a Plan Apochromat 63x 1.4 NA oil objective. The 488 nm line of the Ar ion laser was used for excitation of EGFP. The laser power was maintained at 1% throughout the experiment with the emission collected through a 493-556 nm filter.

B. Cellular Imaging and Analysis

Investigation of peripheral protein association with cellular membranes requires fluorescent labeling of the protein of interest and a technique that can scan fast enough to detect the fluorescent protein in different pixels of an image. RICS is a good method for meeting these objectives as the scanning movement creates a space-time matrix of pixels within each image. From the stack of frames collected for a live cell a spatial correlation map can be obtained to determine the particle's diffusion coefficient. Thus, when the spatial correlation map is obtained at different subcellular location the diffusion coefficient can be determined at different cellular sites. This provides information on how the membranes, organelles, or other cellular components restrict the movement of fluorescently labeled proteins. On commercial confocal microscopes the spatial and temporal sampling time of the laser beam (pixel dwell time) is known as is the scan time between scan lines and time between images. Thus, using RICS allows for generation of spatial-temporal maps of dynamics occurring across the living cell. RICS data was acquired on a commercial laser scanning confocal microscope (Zeiss LSM 710 inverted microscope) using a Plan Apochromat 63x 1.4 NA oil objective. The 488 nm line of the Ar ion laser was used for excitation of EGFP. The laser power was maintained at 1% throughout the experiment with the emission collected through a 493-556 nm filter. The data were collected as images of 256 × 256 pixels with a pixel dwell time of 12.6 μs. RICS analysis was done with SimFCS software using 100 frames from the series of images (Adu-Gyamfi *et al*., 2012).

C. Imaging and Analysis at the Plasma Membrane

In order to more carefully and selectively image VP40 assembly on the inner leaflet of the plasma membrane total internal relfection microscopy (TIRF) imaging was employed (Adu-Gyamfi *et al.*, 2012; Adu-Gyamfi *et al.*, 2013). TIRF imaging was performed using a homebuilt TIRF imaging system (model No. IX81 microscope (Olympus, Melville, NY) as described previously (Ross *et al.*, 2011). Briefly, images were collected using a Cascade 512B EMCCD camera. Samples were excited with the 488 nm line from an Ar ion laser (Melles Griot, Albuquerque, NM) through a 60x, 1.45 NA oil objective (Olympus). To

ensure cell integrity, cells were maintained at 37°C using a thermostated stage (Tokai Hit, Shizuoka, Japan). Images were collected at 256 × 256 pixels with a 50 ms exposure time per frame with 4000 total frames collected. Images were saved as 16 bit unsigned and imported into the SimFCS software (Laboratory for Fluorescence Dynamics, Irvine, CA). TIRF image series were analyzed using SimFCS (Laboratory for Fluorescence Dynamics, Irvine, CA). For N&B analysis 512 frames were analyzed per image series. HEK293 cells expressing monomeric EGFP were used as a brightness standard and were imaged under the same conditions as EGFP-VP40 and respective mutations (See Figure 1).

The brightness of the EGFP was used as the brightness of the monomer as described previously (Adu-Gyamfi *et al.*, 2012) where the average brightness of a monomer was 0.104. This allowed for selection of oligomeric size based upon multiple of the monomer (See Figure 1 and 2). Thus, the selection window for each species is based upon the average brightness, which will yield an average population of each species in the respective area of analysis (See Figure 1 and 2).

III. Considerations

Cells and organelles are dynamic molecules and move during the scanning periods. To counter this issue RICS analysis was performed with a moving average of ten frames in the SimFCS software. This method can account for motions of cells or organelles that are on the timescale of 10 s or longer. Fluorophores can bleach and although RICS analysis is independent of bleaching (because the correlation is determined in each frame), bleaching in N&B analysis can lead to problematic data even with changes as small as 10% of the average intensity. Bleaching was verified for each experiment and didn't exceed 5% of the original intensity in analyzed samples. It is also important to note that N&B analysis accounts for limitations such as autofluorescence, scattering, bright immobile particles, or fast moving particles that are dim by calculating the total variance. Variance is proportional to the particle brightness for particles fluctuating in the focal volume, however, the variance of the immobile particles, scattering, autofluorescence, and detector noise is proportional to the intensity of these components. Thus, only fluorescent fluctuations that are dependent upon the mobile particles have a ratio of the variance to intensity > 1. Brightness maps then allow for pixel resolution of the clustering of fluorescently labeled proteins (See Figure 1 and 2).

It's also important to consider that a fluorescent molecule can move faster than the scanner during line scanning (Digman *et al.*, 2013). This would mean that fast moving particles wouldn't be counted accurately and the average diffusion coefficient would be lower than the true diffusion coefficient. Digman and colleagues recommend keeping the pixel time faster and pixel size larger to detect the fast moving particles before the next line scan (Digman *et al.*, 2013). Typical settings of a pixel size of 0.05 μm and a slow pixel dwell time (25 μs) can detect particles diffusing in cells with diffusion coefficients of ~ 20 $\mu m^2/s$ (Digman *et al.*, 2013). The spatial resolution of RICS is usually larger than the size of a diffraction limited area but smaller than the entire cellular cytoplasm meaning multiple boxes around a cell can be examined independently. This is advantageous for collecting large data sets from single or multiple cell measurements, which is especially important

when determining N&B of particles or the molecular stoichiometry of a protein complex (Digman *et al*., 2009).

IV. Summary and Conclusion

RICS and number and brightness analysis (N&B) are used to monitor the diffusion of fluorescently labeled molecules in live cells or in solution. Together, they can measure the formation of protein oligomers and their stoichiometry while determining the number of molecules that are both free and in complexes. These techniques are advantageous for studying oligomerization in live cells as harsh conditions don't have to be used to lyse the cells and assess oligomerization. Imaging fluorescent fluctuations also doesn't require the large sample size that would be required for performing size exclusion chromatography with multiangle light scattering, which can accurately determine oligomerization state (Wyatt, 1998). Of course, creating fusion proteins with fluorescent tags can influence cellular membrane binding or oligomerization so independent methods should be employed to verify that tagged and untagged proteins behave similarly. This approach has been useful and informative for investigating the basis of assembly and oligomerization of the Ebola virus matrix protein VP40, which regulates egress of the virus from human cells (Adu-Gyamfi *et al*., 2012; 2013).

Oligomerization of VP40 is a critical step in the assembly and replication of the Ebola virus. Inhibition of this step of the viral life cycle has been found to downregulate the formation and release of new virus (Hoenen *et al*., 2010). N&B analysis demonstrated that although oligomers of VP40 were detected on the plasma membrane the majority of plasma membrane associated VP40 was monomeric (See Figure 1 and 2) (Adu-Gyamfi *et al*., 2012). This was not particularly surprising as the monomers may continuously be recruited from the cytosol to serve as building blocks for self-multimerization into larger structures required for membrane bending and plasma membrane egress. We also observed that oligomers (hexamers, octamers, and larger oligomers) were found enriched at the tips of the cells in filamentous protruding structures (See Figure 2) (Adu-Gyamfi *et al*., 2012; 2013). Filamentous protrusion sites are thought to be the sites of egress for Ebola and other filamentous viruses such as Marburg. N&B analysis of an oligomerization deficient mutation supported this notion as when oligomerization was reduced, detectable membrane protrusion sites were no longer observed (Adu-Gyamfi *et al*., 2012; 2013).

N&B analysis can also be applied to peripheral protein interactions *in vitro*. Cho and colleagues have used giant unilamellar vesicles (GUVs) to investigate the oligomerization of BAR and ENTH domains (Yoon *et al*., 2010; 2012) on the surface of membranes. Here they were able to observe large oligomeric complexes that are required to induce membrane tubulation from GUVs (See Figure 3).

Multiple fluorophores also can be used in live cells and provide a robust opportunity to dissect molecular complexes with the RICS and N&B methods (Digman *et al*., 2009; 2013), which would be a boon to monitoring protein-protein interactions or oligomerization induced by lipid membranes. This method has already been applied to resolve the interactions between endophilin and dynamin in live cells (Digman *et al*., 2013).

In closing, raster scanning allows for stacks of images to be generated to study assembly of fluorescently labeled proteins or observation and stoichiometry of complexes to be determined when two or more fluorescently labeled molecules are used. Because fluorescent fluctuation analysis is performed among pixels and frames in a long scan, data on particle diffusion, number of fluorescent molecules in a pixel, and their brightness can be determined. Perhaps most notably, these types of data can be collected on commercial laser scanning microscopes sans modification of the hardware or software. The growing availability of these commercial instruments in core facilities may increase use of the discussed biophysical analysis to study and understand molecular interactions and biological processes occurring on cellular membranes

Acknowledgments

I would like to thank Emmanuel Adu-Gyamfi, Enrico Gratton, and Michelle A. Digman for helpful discussions and their contributions to the original work. Research in the Stahelin lab is supported by the NIH (AI081077), NSF (7112361), and American Heart Association (GRNT12080254).

References

Adu-Gyamfi E, Digman MA, Gratton E, Stahelin RV. Investigation of Ebola VP40 assembly and oligomerization in live cells using the number and brightness analysis. Biophysical Journal. 2012; 102:2517–2525. [PubMed: 22713567]

Adu-Gyamfi E, Soni SP, Xue Y, Digman MA, Gratton E, Stahelin RV. The Ebola virus matrix protein penetrates into the plasma membrane: a key step in viral protein 40 (VP40) oligomerization and viral egress. Journal of Biological Chemistry. 2013; 288:5779–5789. [PubMed: 23297401]

Barnwal RP, Devi KM, Agarwal G, Sharma Y, Chary KV. Temperature-dependent oligomerization in M-crystallin: lead or lag toward cataract, an NMR perspective. Proteins. 2011; 79:569–580. [PubMed: 21117061]

Berland KM, So PT, Gratton E. Two-photon fluorescence correlation spectroscopy: Method and application to the intracellular environment. Biophysical Journal. 1995; 68:694–701. [PubMed: 7696520]

Bertaneli V, Petrov EP, Schwille P. The role of lipids in VDAC oligomnerization. Biophysical Journal. 2012; 102:523–531. [PubMed: 22325275]

Choi CK, Zareno J, Digman MA, Gratton E, Horwitz AR. Cross-correlated fluctuation analysis reveals phosphorylation-regulated paxillin-FAK complexes in nascent adhesions. Biophysical Journal. 2011; 100:583–592. [PubMed: 21281572]

Crosby KC, Postma M, Hink MA, Zeelenberg CHC, Adjobo-Hermans MJW, Gadella TWJ. Quantitative analysis of self-association and mobility of annexin A4 at the plasma membrane. Biophysical Journal. 2013; 104:1875–1885. [PubMed: 23663830]

Digman MA, Brown CM, Sengupta P, Wiseman PW, Horwitz AR, Gratton E. Measuring fast dynamics in solutions and cells with a laser scanning microscope. Biophysical Journal. 2005a; 89:1317–1327. [PubMed: 15908582]

Digman MA, Brown CM, Horwitz AR, Mantulin WW, Gratton E. Paxillin dynamics measured during adhesion assembly and disassembly by correlation spectroscopy. Biophysical Journal. 2008a; 94:2819–2831. [PubMed: 17993500]

Digman MA, Dalal R, Horwitz AF, Gratton E. Mapping the number of molecules and brightness in the laser scanning microscope. Biophysical Journal. 2008b; 94:2320–2332. [PubMed: 18096627]

Digman MA, Gratton E. Analysis of diffusion and binding in cells using the RICS approach. Miscroscopy Research and Technique. 2009; 72:323–332.

Digman MA, Sengupta P, Wiseman PW, Brown CM, Horwitz AR, Gratton E. Fluctuation correlation spectroscopy with a laser-scanning microscope: Exploiting the hidden time structure. Biophysical Journal. 2005b; 88:L33–L36. [PubMed: 15792971]

Digman MA, Stakic M, Gratton E. Raster image correlation spectroscopy and number and brightness analysis. Methods in Enzymology. 2013; 518:121–144. [PubMed: 23276538]

Digman MA, Wiseman PW, Choi C, Horwitz AR, Gratton E. Stoichiometry of molecular complexes at adhesions in living cells. Proceedings of the National Academy of Sciences of the United States of America. 2009; 106:2170–2175. [PubMed: 19168634]

Hoenen T, Jung S, Herwig A, Groseth A, Becker S. Oligomerization of Ebola virus VP40 is essential for particle morphogenesis and regulation of viral transcription. Journal of Virology. 2010; 84:7053–7063. [PubMed: 20463076]

Klein DE, Lee A, Frank DW, Marks MS, Lemmon MA. The pleckstrin homology domain of dynamin isoforms require oligomerization for high affinity phosphoinositide binding. Journal of Biological Chemistry. 1998; 273:27725–27733. [PubMed: 9765310]

Lemmon MA. Membrane recognition by phospholipid-binding domains. Nature Reviews in Molecular and Cellular Biology. 2008; 9:99–111.

Magde D, Elson E, Webb WW. Thermodynamic fluctuations in a reacting system – Measurement by fluorescence correlation spectroscopy. Physical Review Letters. 1972; 29:705–708.

Magde D, Elson E, Webb WW. Fluorescence correlation spectroscopy. II. An experimental realization. Biopolymers. 1974; 13:29–61. [PubMed: 4818131]

Murray PS, Li Z, Wang J, Tang CL, Honig B, Murray D. Retroviral matrix domains share electrostatic homology: models for membrane binding function throughout the viral life cycle. Structure. 2005; 13:1521–1531. [PubMed: 16216583]

Ross JA, Digman MA, Wang L, Gratton E, Albanesi JP, Jameson DM. Oligomerization state of dynamin 2 in cell membranes using TIRF and number and brightness analysis. Biophysical Journal. 2011; 100:L15–L17. [PubMed: 21281565]

Rossow MJ, Sasaki JM, Digman MA, Gratton E. Raster image correlation spectroscopy in live cells. Nature Protocols. 2010; 5:1761–1774.

Schwille P, Bieschke J, Oehlenschläger F. Kinetic investigations by fluorescence correlation spectroscopy: the analytical and diagnostic potential of diffusion studies. Biophysical Chemistry. 1997; 66:211–228. [PubMed: 9362560]

Schwille P, Korlach J, Webb WW. Fluorescence correlation spectroscopy with single molecule sensitivity on cell and model membranes. Cytometry. 1999; 36:176–182. [PubMed: 10404965]

Soni SP, Adu-Gyamfi E, Yong SS, Jee CS, Stahelin RV. The Ebola virus matrix protein deeply penetrates the plasma membrane: an important step in viral egress. Biophysical Journal. 2013; 104:1940–1949. [PubMed: 23663837]

Stahelin RV. Lipid binding domains: more than simple lipid effectors. Journal of Lipid Research. 2009; 50:S299–S304. [PubMed: 19008549]

Wang X, Graveland-Bikker JF, de Kruif CG, Robillard GT. Oligomerization of hydrophobin SC3 in solution: from soluble state to self-assembly. Protein Science. 2004; 13:810–821. [PubMed: 14978312]

Wyatt PJ. Submicromolar particle sizing by multiangle light scattering following fractionation. Journal of Colloid Interface Science. 1998; 197:9–20. [PubMed: 9466838]

Yeung T, Terebiznik M, Yu L, Silvius J, Abidi WM, Phillips M, Levine T, Kapus A, Grinstein S. Receptor activation alters inner surface potential during phagocytosis. Science. 2006; 313:347–351. [PubMed: 16857939]

Yoon Y, Tong J, Lee PJ, Albanese A, Bhardwaj N, Källberg M, Digman MA, Lu H, Gratton E, Shin YK, Cho W. Molecular basis of the potent membrane-remodeling activity of the Epsin 1 N-terminal homology domain. Journal of Biological Chemistry. 2010; 285:531–540. [PubMed: 19880963]

Yoon Y, Zhang X, Cho W. Phosphatidylinositol 4,5-bisphosphate (PtdIns(4,5)P_2) specifically induces membrane penetration and deformation by Bin/Amphiphysin/Rvs (BAR) domains. Journal of Biological Chemistry. 2012; 287:34078–34090. [PubMed: 22888025]

Zimmerberg J, Kozlov MM. How proteins produce cellular membrane curvature. Nature Reviews in Molecular and Cellular Biology. 2006; 7:9–19.

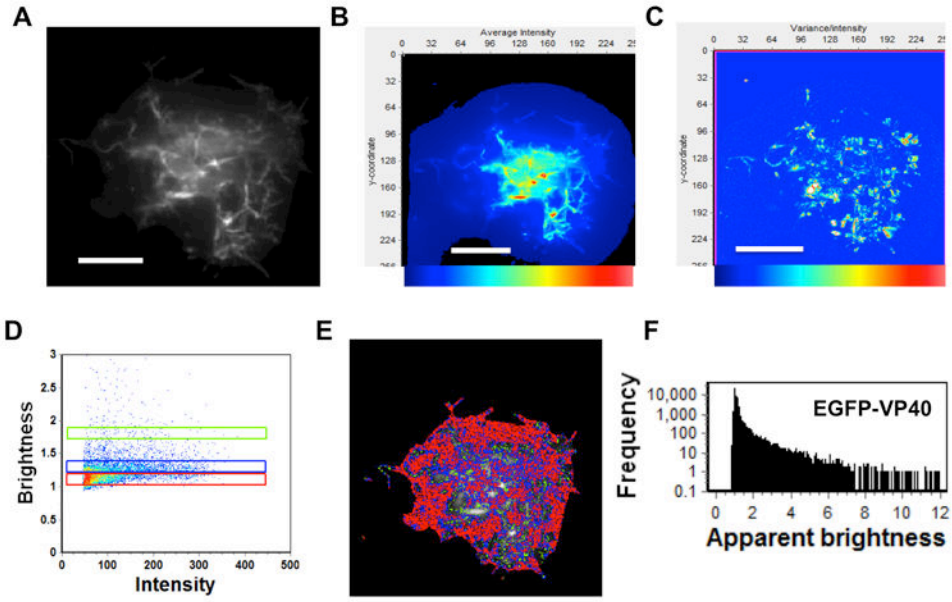

Fig. 1.

Brightness analysis of VP40 in HEK293 cells. A. Membrane protrusion sites emanating from the PM were inspected with TIRF microsopy. B. TIRF average intensity image of a HEK293 cell transfected with plasmid expressing EGFP demonstrates sites of signal enrichment and a number of sites of membrane protrusions and viral egress. C. Brightness image (variance/intensity) of the same cell demonstrates the enriched sites of VLP egress where significant EGFP signal (red) is detected. D. Brightness vs. intensity plot displaying monomers (brightness of 1.104) (red box), dimers (blue box), and hexamers (green box). E. Brightness distribution of VP40 with selected pixels from D displaying localization of monomers (red), dimers (blue), and hexamers (green). F. Frequency versus apparent brightness plot demonstrates the extensive oligomerization of VP40 at or near the PM of HEK293 cells. The apparent brightness of a monomer is 1.104 indicating the significant frequency of a monomer but extensive enrichment of oligomers up to an apparent brightness of 12. Scale bar = 18 μm. This research was originally published in the *Journal of Biological Chemistry*. Emmanuel Adu-Gyamfi, Smita P. Soni, Yi Xue, Michelle A. Digman, Enrico Gratton, and Robert V. Stahelin. The Ebola Virus Matrix Protein Penetrates into the Plasma Membrane: A Key Step in Viral Protein 40 (VP40) Oligomerization and Viral Egress. *J. Biol. Chem.* 2013; 288:5779-5789.

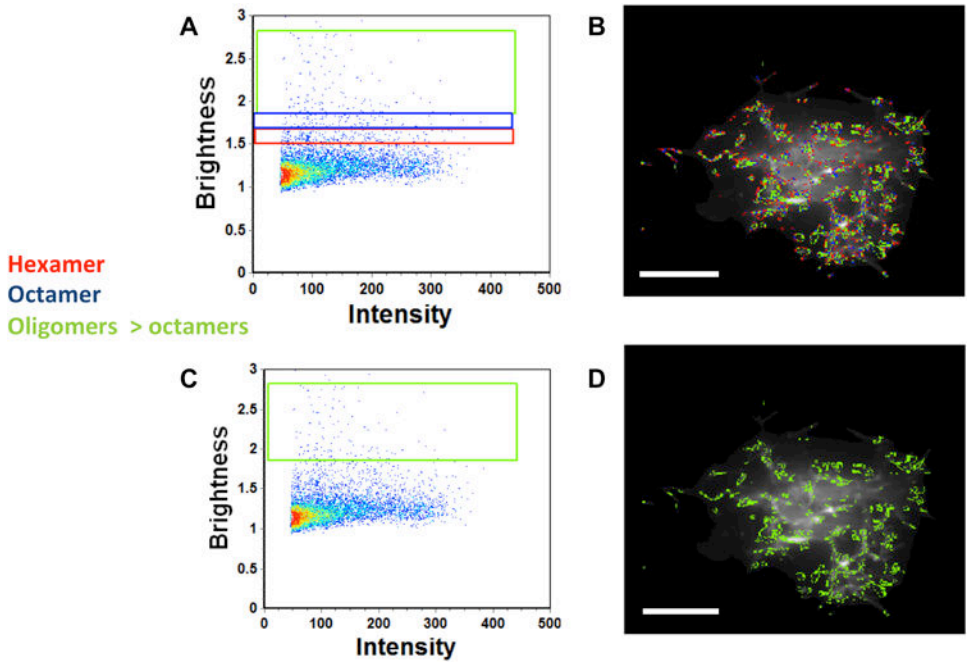

Fig. 2.

Brightness versus intensity analysis of EGFP-VP40 in HEK293 cells displaying oligomers. A. Brightness vs. intensity plot of the HEK293 cell shown in Figure 1 highlighting hexamers (red box), octamers (blue box), and oligomers larger than octamers (green box). B. Brightness distribution of VP40 with selected pixels from A displaying hexamer (red), octamers (blue), and oligomers larger than octamers (green). Oligomeric VP40 structures are enriched on the PM and filaments protruding from the cell PM. C. Brightness vs. intensity plot of the HEK293 cell shown in Figure 4 highlighting oligomers larger than octamers (green box). D. Brightness distribution of VP40 with selected pixels from C displaying oligomers larger than octamers (green). Scale bar = 18 μm. This research was originally published in the *Journal of Biological Chemistry*. Emmanuel Adu-Gyamfi, Smita P. Soni, Yi Xue, Michelle A. Digman, Enrico Gratton, and Robert V. Stahelin. The Ebola Virus Matrix Protein Penetrates into the Plasma Membrane: A Key Step in Viral Protein 40 (VP40) Oligomerization and Viral Egress. *J. Biol. Chem.* 2013; 288:5779-5789.

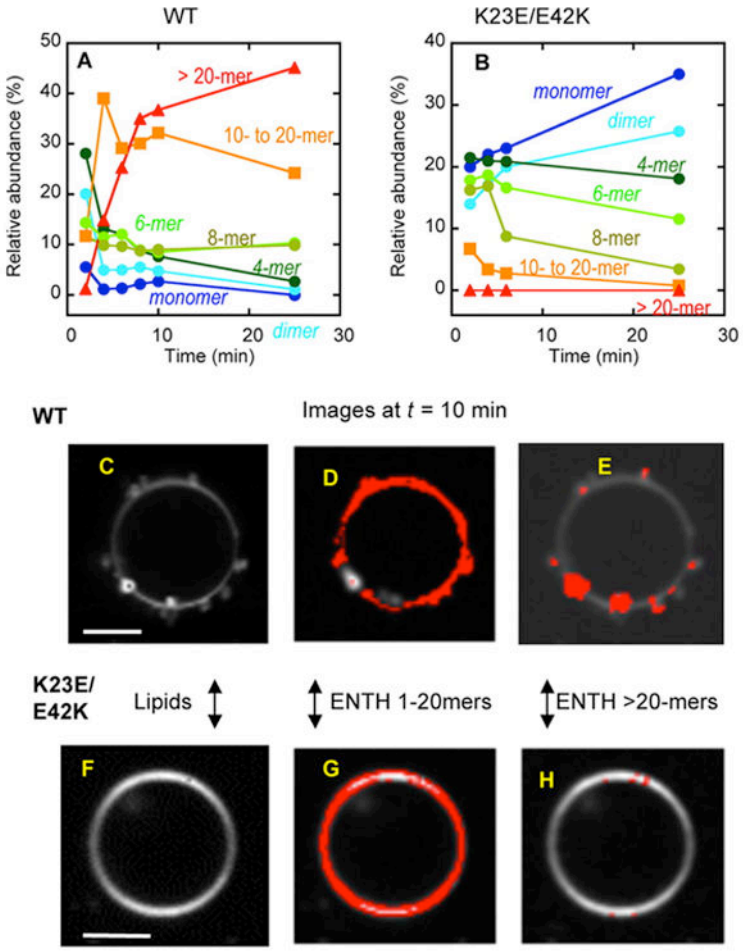

Fig. 3.

Number and brightness analysis of raster-scanned images of GUV tubulation by ENTH domain. A, the time course of the relative abundance of different aggregates for epsin 1 ENTH WT. B, the time course of the relative abundance of different aggregates for epsin ENTH K23E/E42K mutant. C, a representative image of POPC/POPE/POPS/ PtdIns(4,5)P_2/Rh-PE GUV shown by Rh-PE fluorescence after a 10-min treatment with epsin 1 ENTH WT. D, distribution of ENTH WT aggregates (monomer to 20-mer) was superimposed onto the image of GUV. E, distribution of ENTH WT aggregates (>20-mer) was superimposed onto the image of GUV. F, a representative image of POPC/POPE/POPS/ PtdIns(4,5)P_2/Rh-PE GUV after a 10-min treatment with epsin 1 ENTH K23E/E42K. G, distribution of ENTH K23E/E42K (monomer to 20-mer) was superimposed onto the image of GUV. H, distribution of ENTH K23E/E42K aggregates (>20-mer) was superimposed onto the image of GUV. All measurements were performed at 37 °C using POPC/POPE/ POPS/PtdIns(4,5)P_2/Rh-PE (46.5:30:20:3:0.5) GUV in 20 mm Tris-HCl buffer, pH 7.4, with 0.16 m KCl solution. Protein concentration was 0.5 μm. White bars, 10 μm. This research was originally published in the Journal of Biological Chemistry. Youngdae Yoon, Jiansong Tong, Park Joo Lee, Alexandra Albanese, Nitin Bhardwaj, Morten Källberg, Michelle A. Digman, Hui Lu, Enrico Gratton, Yeon-Kyun Shin, and Wonhwa Cho. Molecular Basis of

the Potent Membrane-remodeling Activity of the Epsin 1 N-terminal Homology Domain. *J. Biol. Chem*. 2010; 285:531-540.